Journal of Analysis and Testing (2023) 7:16–24
https://doi.org/10.1007/s41664-022-00246-8

ORIGINAL PAPER

Incorporation of Fluorescent Carbon Quantum Dots into Metal–Organic Frameworks with Peroxidase-Mimicking Activity for High-Performance Ratiometric Fluorescent Biosensing

Qiuyu Ye[1] · Tao Dai[1] · Jin Shen[1] · Qin Xu[1] · Xiaoya Hu[1] · Yun Shu[1]

Received: 5 October 2022 / Accepted: 12 November 2022 / Published online: 22 December 2022

Abstract
A new ratiometric fluorescent sensor based on the bifunctional carbon quantum dots (CQDs)@metal–organic framework (MOF) nanocomposite possessing peroxidase-mimicking catalytic and luminescent characteristics was developed for hydrogen peroxide (H_2O_2) and cholesterol detection. The incorporation of fluorescent CQDs into the cavities of MIL-101(Fe) MOF with peroxidase-like activities endows the nanocomposite with bifunctional properties. The CQDs@MOF can oxidize *o*-phenylene-diamine to 2,3-diaminophenolazine by H_2O_2 with yellow fluorescence (556 nm). Meantime, the intrinsic fluorescence signal (455 nm) of CQDs@MOF is inhibited due to the inner filter effect. Therefore, the ratio of the fluorescent intensity is employed as the signal output to construct the H_2O_2 ratiometric biosensor. In addition, the cholesterol can be determined by the ratiometric sensor with high sensitivity. In addition, the total cholesterol in human serum is determined with high accuracy using our ratiometric biosensor. This ratiometric fluorescent platform based on the bifunctional CQDs@MOF provides new insights in the field of bio-sensing.

Keywords Carbon quantum dots · Metal–organic framework · Peroxidase-like activity · Ratiometric fluorescent detection

1 Introduction

Cholesterol (Chol) is the most important sterol produced by human cells and an important metabolite that reflects the health condition of the human body [1]. Furthermore, Chol is a core member of cell membranes and a precursor of many biomolecules, such as anabolic steroids, bile acids and vitamin D. The total Chol (TC) content is commonly composed of free cholesterol (about 30%) and cholesterol esters (about 70%) in human serum [2]. It has been shown that Chol can be converted to hydrogen peroxide (H_2O_2) in the presence of cholesterol oxidase (ChOx). To date, various techniques, including absorption spectroscopy [3, 4], electrochemistry [5, 6], fluorescence [7], chemiluminescence [8, 9] and liquid chromatography [10], have been used for the detection of H_2O_2. The fluorescence detection has been widely used due to its unique advantages, such as high sensitivity, high accuracy and simplicity [11–14]. However, fluorescent sensing methods that rely on single signal response are more susceptible to be affected by many environmental factors in detection environment. The ratiometric sensor based on dual-emission fluorescent probe can effectively eliminate the influence of detection instrument and environment to reduce the error response and improve the accuracy of signal response [7, 15, 16]. Therefore, the construction of a dual-emission fluorescent probe is of great significance for the reliable detection of H_2O_2.

Metal–organic framework (MOF) is a kind of mixed organic and inorganic crystalline material, which has been widely used in catalysis field because of its large specific surface area, adjustable porosity and a large number of exposed active sites [17–19]. In recent years, some MOF materials with redox metal nodes have peroxidase-mimetic catalytic activity similar to biological enzymes [20–23]. Such as MIL-53 (Fe) [24], MIL-88 (Fe) [25], MIL-101 (Fe) [26] and Fe-based MOFs with peroxidase-mimetic catalytic ability [27, 28], can catalyze H_2O_2 reaction, oxidize 3,3′,5,5′-tetramethylbenzidine (TMB), *o*-phenylene-diamine (OPD) and other chromogenic reagents, resulting in color reaction. At the same time, the stability of MOF nano-enzyme can break

✉ Yun Shu
shuyun@yzu.edu.cn

[1] School of Chemistry and Chemical Engineering, Yangzhou University, Yangzhou 225002, China

through the limitations brought by the environment. The adjustable porosity of MOFs provides a rich space for the introduction of luminescent guests, affording an excellent platform for the construction of luminescent sensors. Compared with the luminescence of MOF which mainly comes from ligands, introducing the luminescent guests through post-modification synthesis shows more fluorescence diversity and tunability. Fluorescent carbon quantum dots (CQDs) can be considered as good luminescent guest with many advantages, such as facile synthesis, easy functionalization, good dispersibility, stable photochemical properties and good biocompatibility [29–32]. However, CQDs are easy to agglomerate. Loading carbon dots into the MOF cavity can avoid agglomeration and ensure the fluorescence stability of CQDs effectively [33, 34].

Here, we design and construct a new ratiometric fluorescent biosensor based on the CQDs loading iron-based organic framework (CQDs@MIL-101(Fe)) nanocomposite with fluorescent and peroxidase-like catalytic characteristics (Scheme 1). After post-modification and incorporation of fluorescent CQDs, the nanocomposite shows blue fluorescence at 455 nm, and the Fe^{3+}/Fe^{2+} redox pair in MOF makes it possess good peroxidase-mimicking activity. With the participation of CQDs@MOF, OPD can be oxidized to 2,3-diaminophenosine (DAP) by H_2O_2 with significant yellow fluorescence at 575 nm. Due to the strong absorption of DAP at about 450 nm, the fluorescence inner filter effect (IFE) between DAP and CQDs@MOF (455 nm) can significantly inhibit the blue fluorescence signal of the nanocomposite. While, the yellow fluorescence of the product DAP significantly enhanced with the increase of H_2O_2 concentration. So the ratio fluorescence detection of H_2O_2 can be achieved. As cholesterol can be hydrolyzed by cholesterol oxidase to produce H_2O_2, the ratiometric fluorescent sensor also can be used for the determination of cholesterol. Finally, the detection of TC in serum samples was achieved using the bifunctional nanocomposite-based ratiometric fluorescent sensor.

2 Experimental

2.1 Materials

$FeCl_3·6H_2O$, ethylene-diamine, *N*,*N*-dimethyl-formamide (DMF), H_2O_2 (30%), ethanol, methanol, glutathione (GSH), ascorbic acid (AA), dopamine (DA), cysteine (Cys), glucose (Glu) and serine (Ser) were bought from Sinopharm Chemical Reagent Co., Ltd. (Shanghai, China). 1,4-dicarboxybenzene (H_2BDC), cholesterol and citric acid were bought from Aladdin Reagent Co., Ltd. (Shanghai, China). Cholesterol oxidase and cholesteryl ester oxidase were purchased from Yuanye Bio-Technology Co., Ltd. (Shanghai, China).

2.2 Synthesis of CQDs

CQDs were synthesized directly by a hydrothermal method [35]. In brief, citric acid (1.0507 g) and ethylene-diamine (335 μL) were dissolved in deionized water (10 mL) and stirred for 30 min. The precursor was then transferred to a Teflon-lined stainless steel autoclave (25 mL) and heated at 200 ℃ for 5 h. CQDs aqueous solution with good dispersion was obtained after the reactor cooling to room temperature naturally. The solution was then purified by a dialysis membrane (500 MWCO) for 24 h.

2.3 Synthesis of MIL-101(Fe)

Using a one-pot solvothermal method, MIL-101(Fe) was prepared [36]. $FeCl_3·6H_2O$ (1.350 g) and H_2BDC (0.412 g)

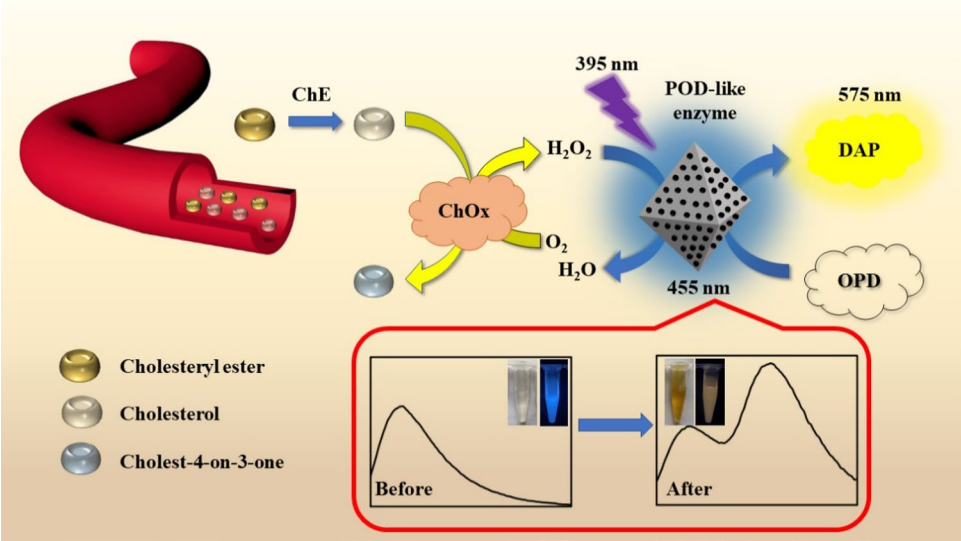

Scheme 1 Schematic representation of the fluorescent ratiometric sensor based on bifunctional CQDs@MIL-101(Fe) nanocomposite for cholesterol detection

were added into DMF (30 mL) and magnetically stirred for 30 min. The solution was switched to a Teflon-lined stainless steel autoclave (50 mL) and heated at 110 °C for 20 h. After cooling, the mixture was centrifuged and washed with DMF and ethanol, respectively. Then, the organic ligand in the frame was removed with methanol solvent for 24 h by the Soxhlet extraction method [37]. Finally, the resultant solids were dried in a vacuum oven at 60 ℃.

2.4 Preparation of CQDs@MOF

CQDs@MOF nanocomposite was prepared as follows: the solution inside the dialysis bag was diluted with ultrapure water to 10 mL and prepared CQDs solution. 1 mL CQDs solution, 10, 30, 50, and 100 mg MIL-101 (Fe) powder, and 10 mL deionized water were added into a 20 mL glass bottle and then were dispersed evenly by ultrasonic. After magnetic stirring for 48 h, the brown powder was obtained by centrifugation at 10,000 r/min and dried in an oven at 60 ℃ for 24 h. According to the condition optimization results, the bifunctional nanocomposites material synthesized under the addition of 50 mg MIL-101 (Fe) powder was selected for the subsequent detection experiments.

2.5 Materials Characterization

The fluorescence measurement was performed by the spectrofluorometer (FS-5, Edinburgh Instruments, Britain). The crystal structure and morphology analyses of materials were performed by the X-ray powder diffraction (XRD, D8 Advance diffractometer with Cu Kα radiation, Bruker Co., Germany) and the scanning electron microscope (SEM, Zeiss_Supra55, Carl Zeiss AG, Germany), and the morphology analysis of CQDs was observed by the high-resolution transmission electron microscope (HRTEM, Tecnai G2 F30S-TWIN, FEI USA, Inc., USA). Electron paramagnetic resonance (EPR) analysis was conducted using an A300-10/12 EPR spectrometer (Bruker Co., Germany).

2.6 Detection of H_2O_2

100 μL H_2O_2 solutions of different concentrations (10.0, 50.0 μmol/L and 0.1, 0.25, 0.5, 1.0, 2.5, 5.0, 10.0 mmol/L) were added into OPD and composite material solution which dispersed in NaAc-HAc buffer (10 mmol/L, pH 5.0). And then the mixed liquor was oscillated at 37 ℃ for 45 min. The fluorescence spectra of 410–700 nm were measured at 395 nm excitation wavelength.

2.7 Detection of Cholesterol

For selectivity test, 100 μL cholesterol oxidase solution (50 mg/mL) was added into 100 μL of Chol, Glu, Ser, GSH, Cys, DA and AA, respectively, and the mixture liquid was oscillated at 37 ℃ for 1 h. Then 200 μL OPD solution and 200 μL composite solution (0.1 mg/mL), 1400 μL NaAc-HAc buffer (10 mmol/L, pH 5.0) were added, and the mixture liquid was oscillated at 37 ℃ for 45 min. The fluorescence spectra were measured. For sensitivity test, 100 μL cholesterol oxidase solution (50 mg/mL) was added into 100 μL cholesterol solutions of different concentrations (0.1, 0.2, 0.5, 1.0, 1.5, 2.0, 5.0, 10.0 and 20.0 mmol/L), respectively, and the mixture liquid was oscillated at 37 ℃ for 1 h. Then 200 μL OPD solution and 200 μL composite solution (0.1 mg/mL), 1400 μL NaAc-HAc buffer (10 mmol/L, pH 5.0) were added, and the mixture liquid was oscillated at 37 ℃ for 45 min. Then the fluorescence spectra were measured.

2.8 Detection of Cholesterol in Serum Samples

The TC in diluted serum samples was determined by the standard recovery method. 100 μL cholesterol esterase oxidase solution (50 mg/mL) and 100 μL cholesterol oxidase solution (50 mg/mL) were added in 20 μL serum samples, and then the mixture was oscillated at 37 ℃ for 1 h. Then 200 μL OPD solution and 200 μL composite solution (0.1 mg/mL), and 1400 μL NaAc-HAc buffer (10 mmol/L, pH 5.0) were added, and the reaction solution was oscillated at 37 ℃ for 45 min. The fluorescence spectra were determined. Different concentrations (50, 100 and 150 μmol/L) of cholesterol solutions were added to the serum samples, and the test was conducted according to the same experimental operation.

3 Results and Discussion

3.1 Materials Characterization

In this work, MIL-101 (Fe) was synthesized using a facile solvothermal method. To verify the successful preparation of MIL-101 (Fe), the morphology and structure were systematically characterized by SEM, XRD and XPS analysis. The SEM image of Fig. 1a shows the as-synthesized MIL-101 (Fe) presents a spindle shape with a relatively uniform size of 1 μm. After Soxhlet extraction, obvious holes were observed on the surface of the spindle structure, which are favorable for the subsequent loading of CQDs. In Fig. 1b, the size of CQDs is uniform and the clear atomic plane of CQDs shows a d-spacing of 0.34 nm which is consistent with previous reports [35], indicating the successful preparation of CQDs. The multifunctional fluorescent-catalytic nanocomposite of CQDs@MIL-101(Fe) was prepared by introducing fluorescent CQDs into Fe MOFs with peroxidase-like activity. Compared with MIL-101 (Fe), the SEM image of

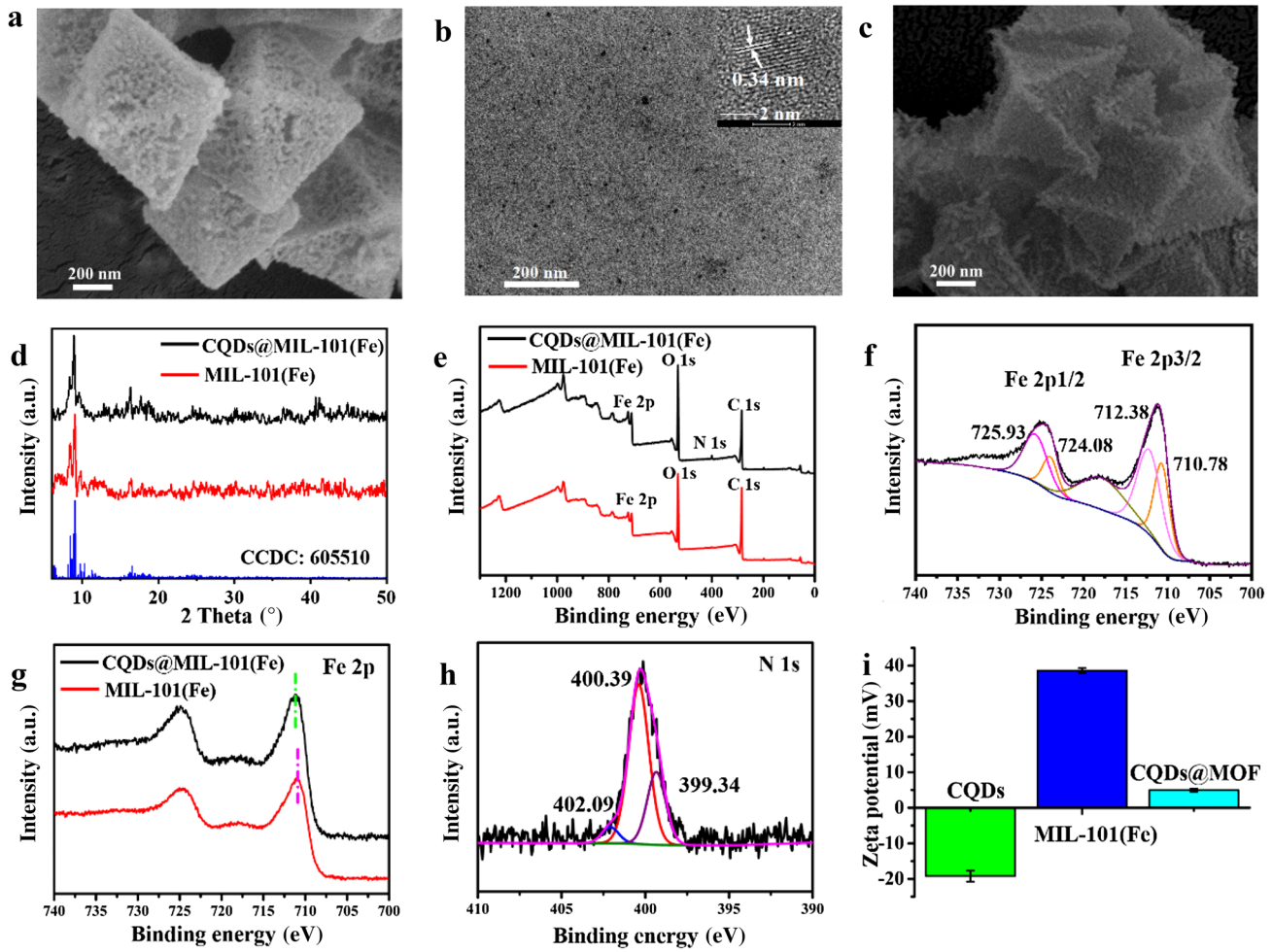

Fig. 1 **a** SEM image of MIL-101 (Fe); **b** TEM image of CQDs; **c** SEM image of CQDs@MOF; **d** XRD patterns of MIL-101 (Fe) and CQDs@MOF; **e** Full scan XPS spectra for MIL-101 (Fe) and CQDs@MOF; **f** XPS spectra of Fe 2p for MIL-101 (Fe); **g** XPS spectra of Fe 2p for MIL-101 (Fe) and CQDs@MOF; **h** XPS spectra of N 1s for CQDs@MOF; **i** Zeta potential of CQDs, MIL-101 (Fe) and CQDs@MOF

MIL-101 (Fe) loading with CQDs shows that most of the holes on the surface were filled (Fig. 1c).

By comparing the XRD characteristic peaks of MOF before and after CQDs loading, it was found that the XRD characteristic peaks of the synthesized MOF material were consistent with that of the simulation of MIL-101 (CCDC: 605510) [36] (Fig. 1d), and there was no change in crystal structure after loading of CQDs, indicating that MOF still keeps its structural integrity. The wide-scan XPS spectra (Fig. 1e) prove that CQDs@MOF is composed of Fe, O, N and C elements, while N element is not observed in MIL-101 (Fe) [38], further validating the loading of CQDs. In addition, the Fe 2p XPS spectra (Fig. 1f) confirm the presence of Fe^{3+} and Fe^{2+} [39]. The peaks of 725.93 and 712.38 eV were corresponded to the 2p spectrum of Fe^{3+}, and the peaks of 724.08 and 710.78 eV were attributed to the 2p spectrum of Fe^{2+}, respectively. The Fe^{3+}/Fe^{2+} redox couple makes MOF possess peroxidase catalytic activity [35]. By comparing the XPS spectra of Fe 2p before and after loading CQDs, it is found that the peak of Fe $2p_{3/2}$ has a weak redshift, which might be caused by electrostatic binding between the CQDs and Fe ions (Fig. 1g). Figure 1h shows three peaks of N 1 s spectra for CQDs@MOF are corresponded to three nitrogen groups: O=C–N (399.34 eV), C–N (400.39 eV) and N–H (402.09 eV) that come from CQDs [40, 41]. Figure 1i shows that the Zeta potential of CQDs and MIL-101 is located at − 19.23 and 38.60 mV, respectively, and the Zeta potential of CQDs@MOF shifts to 4.95 mV after the combination, which proves that the CQDs@MOF complex is formed through electrostatic binding of CQDs and MIL-101 (Fe).

3.2 Study on the Catalytic Activity of Fluorescence CQDs@MOF

Fluorescent CQDs@MOF nanocomposites were obtained by incorporation of CQDs into the MOF matrix. The fluorescence spectrum of the nanocomposite was recorded. As shown in Fig. 2a, CQDs@MOF displays the fluorescence emission peak of 455 nm belonging to CQDs under the excitation wavelength of 395 nm. This shows that the as-prepared CQDs@MOF nanomaterial possesses the photoluminescence properties, and its fluorescence comes from the incorporation of CQDs. Under the excitation of UV lamp (365 nm), CQDs@MOF shows bright blue fluorescence (Fig. 2a inset). To study the peroxidase-mimetic property of CQDs@MOF nanocomposite, it was used to catalyze common H_2O_2 + OPD color reaction. The peroxidase-mimicking characteristics were studied by recording color change of the solution. When CQDs@MOF was added to H_2O_2 + OPD system, the solution changed from colorless to yellow obviously, while the color of other systems does not change (Fig. 2a inset). The color change is caused by the oxidation of colorless OPD to yellow product DAP. It demonstrates that CQDs@MOF has a catalytic activity similar to that of peroxidase, which can catalyze H_2O_2 and then oxidize OPD to DAP. The catalytic activity of CQDs@MOF is mainly attributed to its redox couple of Fe^{3+}/Fe^{2+} [42]. In the cholesterol, ChOx and OPD systems, the results show that the color of the solution also changed, it is because that ChOx could catalyze cholesterol to produce H_2O_2.

It is interesting to find that the catalytic oxidation of OPD by CQDs@MOF could cause the fluorescence change in the whole system. As shown in Fig. 2a, after adding CQDs@MOF to H_2O_2 + OPD, a yellow fluorescence signal appeared at about 575 nm, which was caused by the oxidation of OPD to produce DAP product with yellow fluorescence [43, 44]. Meanwhile, the fluorescence signal of CQDs@MOF at 455 nm is inhibited. To investigate the mechanism of the fluorescent change of the CQDs, the UV–Vis absorption spectra and fluorescence emission spectrum of DAP oxidized from OPD using different amounts of CQDs@MOF were recorded. As shown in Fig. 2b, the absorption spectra of DAP and the fluorescence emission spectrum of CQDs@MOF overlap significantly. With the amount of OPD increasing, the overlap ratio increases. In summary, the quenching effect is mainly caused by the IFE between CQDs@MOF and DAP [39, 45, 46].

To investigate the peroxide-like catalytic oxidation mechanism of H_2O_2 + OPD by CQDs@MOF, possible reaction intermediates were analyzed by the EPR spectroscopy analysis. Typical ·OH signal was observed by EPR analysis (Fig. 2c), indicating that ·OH was formed during the reaction, while there was none O_2^- captured. Therefore, the mechanism that CQDs@MOF catalyzes H_2O_2 to promote the oxidation of OPD is that nanocomposite acts as a peroxide mimicking enzyme to decompose H_2O_2 into ·OH, and then oxidizes OPD substrate to produce DAP with yellow fluorescence signal. Subsequently, the fluorescence spectra of the H_2O_2 + OPD products catalyzed by CQDs@MOF nanocomposites, which were synthesized at different amount of MOF, were recorded. Figure 2d and Fig. S1 show that the fluorescence peak and absorption peak of DAP gradually increased at first and kept stable later with the increase of

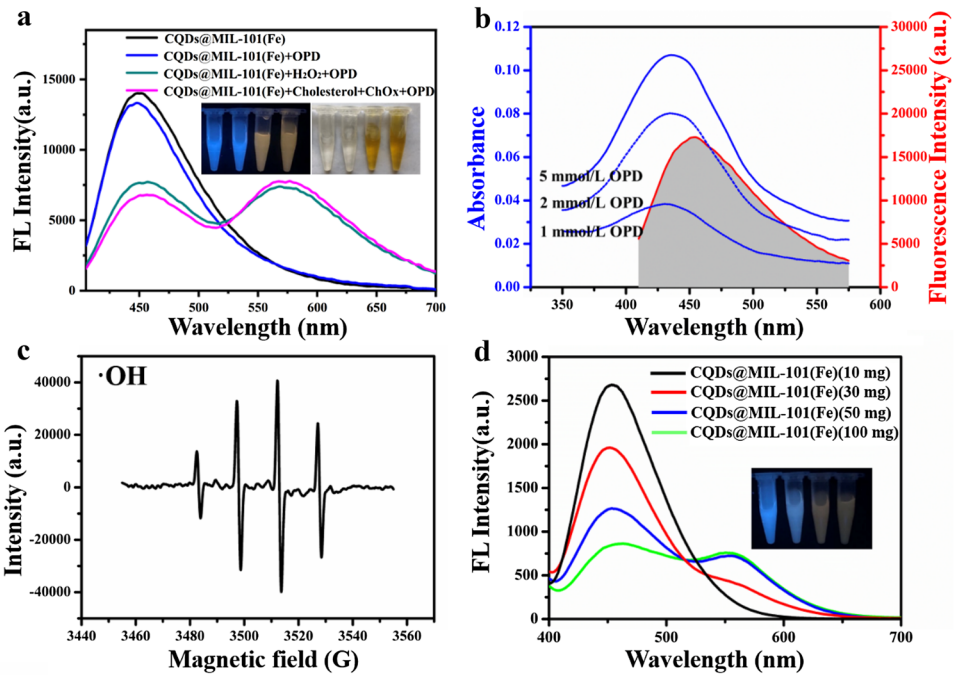

Fig. 2 **a** The fluorescence spectra of CQDs@MOF, CQDs@OF + OPD, CQDs@MOF + OPD + H_2O_2, and CQDs@MOF + OPD + cholesterol + ChOx. Inset: photos of the corresponding solutions under excitation by 365 nm UV lamp; **b** the fluorescence emission spectrum of CQDs@MOF (excitation wavelength: 395 nm) and UV–vis absorption spectra of the product DAP which oxidized from different concentrations of OPD; **c** EPR spectra recorded in the CQDs@MOF + H_2O_2 + DMPO system; **d** fluorescence spectra of CQDs@MOF synthesized under different amount of MIL-101 (Fe) in H_2O_2 + OPD system and the physical images under excitation by 365 nm UV lamp

MOF amount, and the peak intensity reached the maximum when the amount of the MOF increased to 50 mg. It indicated that the peroxidase-mimicking activity of the material reached the highest when the amount of MOF was 50 mg. Therefore, the nanocomposite synthesized under this condition was used for the subsequent studies.

3.3 Detection of H_2O_2 and Cholesterol

Next, the ratiometric fluorescence sensor based on the bifunctional CQDs@MOF nanocomposite was constructed and utilized for detecting H_2O_2 and cholesterol. To obtain the high detection performance for the ratiometric fluorescence sensor, the effects of excitation wavelength, reaction time, pH value and cholesterol oxidase concentration on the ratio fluorescence sensor system were studied. As shown in Fig. S2a, the fluorescence spectra of the mixed system of CQDs@MOF + H_2O_2 + OPD changed with excitation wavelength varying. When the excitation wavelength was set as 405 nm, the fluorescence peak of CQDs was not obvious. However, the fluorescence emission peaks of DAP and CQDs@MOF both showed obvious at the excitation wavelength of 395 nm, which was selected in the following experiment. The reaction time was further optimized, and the fluorescence emission peak intensity of DAP increased gradually with the increase of time and reached equilibrium in 45 min (Fig. S2b). In Fig. S2c, when pH was about 5.0, the composite material showed the strongest peroxidase-like activity to catalyze the oxidation of OPD into DAP. As displayed in Fig. S2d, with the concentration of cholesterol oxidase gradually increased, the amount of H_2O_2 produced by cholesterol oxidation also increased, and more ·OH were generated under the catalysis of CQDs@MOF, leading to the increase of fluorescence intensity for DAP. The optimal catalytic activity can be achieved when the concentration of cholesterol oxidase was 50 mg/mL. Therefore, subsequent experiments were carried out under the optimal reaction conditions mentioned above.

The fluorescence spectra of CQDs@MOF + OPD system after the addition of different concentrations of H_2O_2 were measured under the optimum conditions. As shown in Fig. 3a, the fluorescence peak intensity at 575 nm gradually increased as the concentration of H_2O_2 increased from 0 to 500 μmol/L, while the fluorescence peak intensity at 455 nm gradually decreased. When H_2O_2 concentration is in the range of 2.5–500 μmol/L (Fig. 3b), the fluorescence intensity ratio (I_{575}/I_{455}) with H_2O_2 concentration has a good functioning relationship. This indicates that CQDs@MOF-based ratiometric fluorescence sensor can be used for the quantitative detection of H_2O_2. And the fluorescence intensity ratio I_{575}/I_{455} and H_2O_2 concentration follow a good linear relationship within the concentration range of 2.5–125 μmol/L ($R^2 = 0.9951$). The linear equation can be fitted as follow: $I_{575}/I_{455} = 0.44575 + 0.02633\ c_{H_2O_2}$, and the limit of detection (LOD) is 1.354 μmol/L. Furthermore, the fluorescence spectra of the CQDs@MOF + OPD + ChOx system with different concentrations of cholesterol were measured. The fluorescence peak at 575 nm gradually increased with the

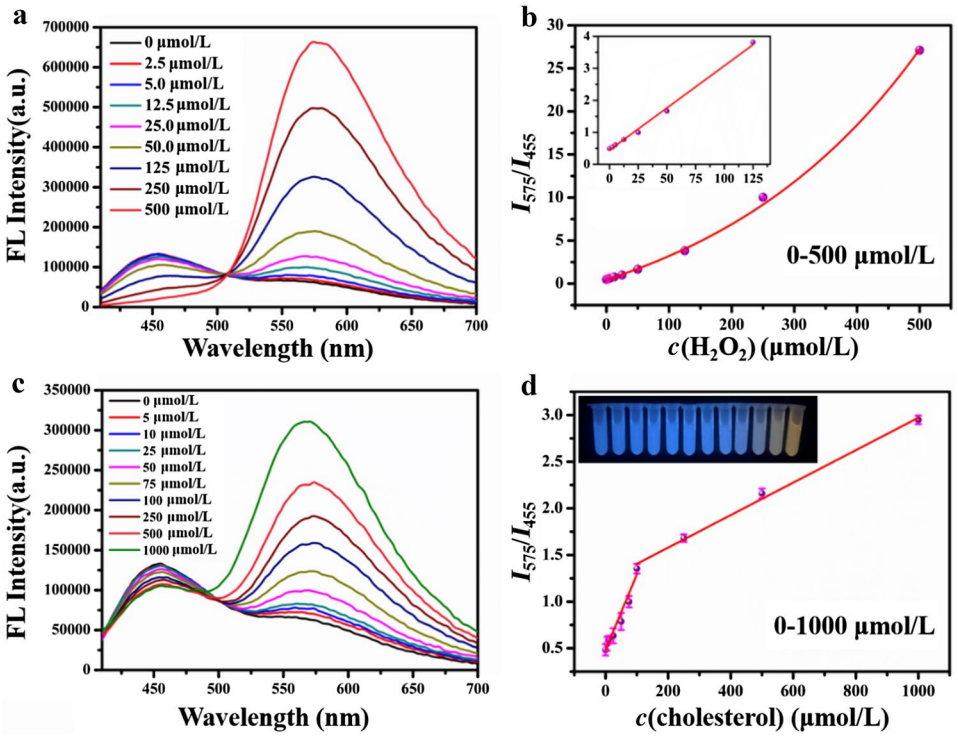

Fig. 3 **a, c** Emission spectra of CQDs@MOF + OPD and CQDs@MOF + OPD + ChOx with different concentrations of hydrogen peroxide and cholesterol. **b, d** Linear graphs of I_{575}/I_{455} at different concentrations of H_2O_2 and cholesterol; inset: fluorescence photos of CQDs@MOF + OPD + ChOx solution after the addition of different concentrations of cholesterol

cholesterol concentration increased from 0 to 1000 μmol/L, while the fluorescence peak at 455 nm gradually weakened (Fig. 3c). As shown in Fig. 3d, the fluorescence intensity ratio (I_{575}/I_{455}) has a good linear relationship with cholesterol concentration in the range of 5–100 μmol/L and 100–1000 μmol/L ($R^2 = 0.9647$ and $R^2 = 0.9940$), respectively. It demonstrates that the dual-function fluorescent ratio probe CQDs@MOF can also be used for the quantitative detection of cholesterol. The LOD for cholesterol is 4.55 μmol/L. Compared with other MOF-based fluorescence sensors for cholesterol detection (Table S1), this sensor shows good detection performance. Therefore, the CQDs@MOF-based ratiometric fluorescent sensor has great application potential in H_2O_2 and cholesterol detection.

To investigate the specificity of the prepared bifunctional CQDs@MOF nanocomposite-based ratiometric fluorescence sensor for cholesterol analysis, the effects of common coexisting substances in serum samples on detection were performed, including reductive substances (GSH, AA and DA), amino acids (Cys and Ser), and sugar (Glu). Figure 4a shows that the intensity of I_{575}/I_{455} changed significantly in the presence of the target cholesterol, while the presence of other substances had little effects on the fluorescence intensity, indicating that the nanocomposite material has good peroxidase-like catalytic activity and high selectivity for cholesterol detection. Subsequently, the anti-interference performance of the fluorescent probe was studied. As seen from Fig. S3 and Fig. 4b, the fluorescence intensity changed same in the presence of other biomolecular interferents as that in the presence of cholesterol only, demonstrating that the presence of these interferents does not affect the detection of cholesterol. Overall, this ratiometric fluorescent sensor based on the bifunctional CQDs@MOF nanocomposite achieves highly specific and accurate detection for H_2O_2 and cholesterol. The main merits of this detection method were discussed as follows: (1) Cholesterol oxidase has a unique ability to hydrolyze cholesterol, and the fluorescent nanocomposite can effectively catalyze the product H_2O_2, so it has a good selectivity. (2) Compared with the fluorescence method based on single emission, this ratiometric fluorescence sensing method can eliminate the influence of other factors caused by the external environment to reduce the error response and improve the accuracy of signal response. (3) The sensor detects cholesterol by measuring the concentration of H_2O_2 in the sample, so other analytes that can be converted to H_2O_2 can also be measured using this sensing system, such as glucose, uric acid and lactic acid.

Finally, the possibility of using the CQDs@MOF-based dual-function ratio-metric fluorescence sensor to analyze TC in actual serum samples was evaluated. The TC level is composed of cholesteryl ester and free cholesterol level. First, the cholesteryl ester was hydrolyzed to cholesterol by ChOx, and then the total free cholesterol level was determined. The serum samples were diluted 100 times with NaAc-HAc buffer to avoid auto-fluorescence interference of serum. As shown in Fig. 4c, d and Table S2, the TC levels in the serum samples of the two normal people were determined as 2.86 and 3.07 mmol/L, respectively, indicating that the TC levels

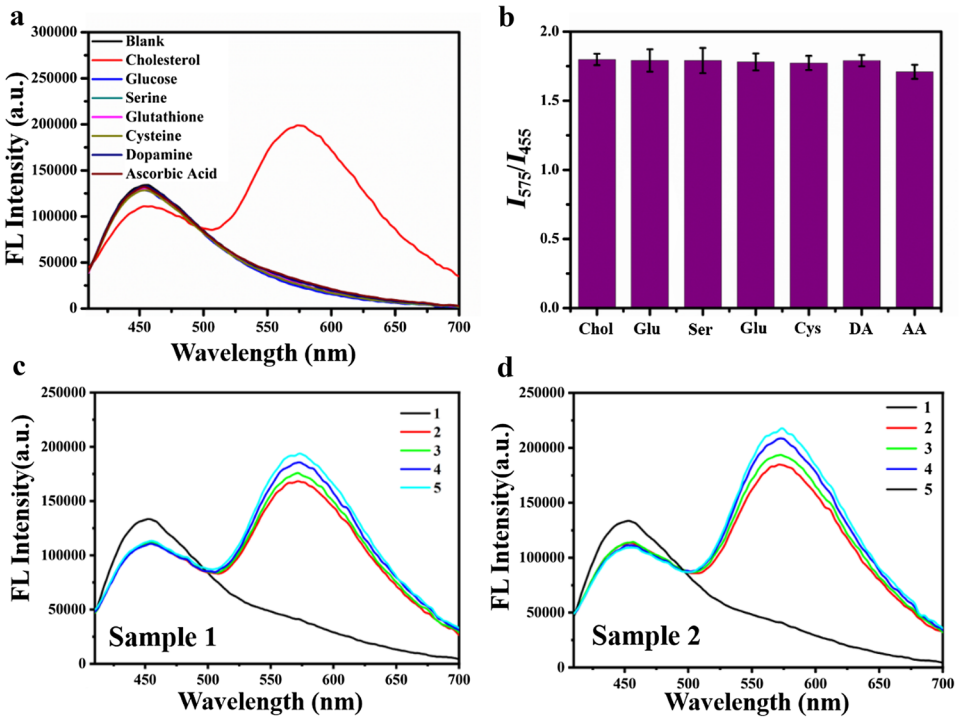

Fig. 4 **a** Fluorescence spectra of CQDs@MOF after the addition of different biomolecules; **b** the I_{575}/I_{455} intensity of the detection system in the presence of cholesterol only and cholesterol coexisting with other biomolecules; **c, d** emission spectra of CQDs@MOF (1), CQDs@MOF and human serum (2), CQDs@MOF and human serum with addition of different concentrations of cholesterol [(3) 50 μmol/L, (4) 100 μmol/L, (5) 150 μmol/L)]

are within the normal range [1, 2]. Then, by adding different standard concentrations of the target substance into the two serum samples, high recovery rates of 95.4–107.0% can be obtained. The above results verify the reliability and accuracy of our designed dual-function fluorescence ratiometric probe in the analysis of TC in real serum samples.

4 Conclusion

In summary, we constructed a ratiometric fluorescent biosensor based on the bifunctional CQDs@MIL-101(Fe) nanocomposite possessing luminescent and peroxidase-mimicking catalytic characteristics for the determination of TC in human serum. On the one hand, the incorporation of fluorescent CQDs into the cavities of MOF endows the nanocomposite with blue fluorescence at 455 nm. On the other hand, the nanocomposite shows high peroxidase-mimicking catalytic activity, which can trigger the oxidation of OPD to DAP by H_2O_2 with yellow fluorescence at 556 nm. Due to the IFE between DAP and the nanocomposite, the inherent fluorescence of nanocomposite was inhibited. The ratio of the fluorescence intensity at 556 and 455 nm was employed as detection signal to construct the H_2O_2 ratiometric biosensing platform. Cholesterol, which can be hydrolyzed by cholesterol oxidase to produce H_2O_2, was also can be determined by the ratiometric fluorescent biosensor with high sensitivity and selectivity. The successful application of the ratiometric fluorescent sensor based on bifunctional CQDs@MOF in cholesterol determination of serum samples validates its application prospect in complex environment analysis. Overall, our work not only establishes a novel ratiometric fluorescence sensing platform with excellent performance, but also provides insights for the rational design of multifunctional MOF nanozymes in the bio-sensing field.

Supplementary Information The online version contains supplementary material available at https://doi.org/10.1007/s41664-022-00246-8.

Acknowledgements We gratefully acknowledge the financial support from the NSFC (21705141, 22076161, 21675140, 21575124), the Green Yang Jinfeng Talent Project of Yangzhou, the High-end talent Support Program of Yangzhou University, and the Interdisciplinary Research Foundation for Chemistry Discipline of Targeted Support of Yangzhou University (yzuxk202009).

Author Contributions QY: Conceptualization, Methodology, Writing-original draft, Formal analysis. TD: Data curation, Methodology. JS: Data curation, Investigation. QX: Visualization, Investigation. XH: Supervision, Funding acquisition. YS: Conceptualization, Supervision, Methodology, Writing–review and editing, Project administration.

Declarations

Conflict of interest The authors declare no competing financial interest.

References

1. Kitchawengkul N, Prakobkij A, Anutrasakda W, Yodsin N, Jungsuttiwong S, Chunta S, Amatatongchai M, Jarujamrus P. Mimicking peroxidase-like activity of nitrogen-doped carbon dots (N-CDs) coupled with a laminated three-dimensional microfluidic paper-based analytical device (laminated 3D-muPAD) for smart sensing of total cholesterol from whole blood. Anal Chem. 2021;93(18):6989.
2. Narwa V, Deswal R, Batra B, Kalra V, Hooda R, Sharma M, Rana JS. Cholesterol biosensors: a review. Steroids. 2019;143:6–17.
3. Xia F, Shi QF, Nan ZD. Facile synthesis of Cu–$CuFe_2O_4$ nanozymes for sensitive assay of H_2O_2 and GSH. Dalton Trans. 2020;49(36):12780–92.
4. Chen JY, Shu Y, Li HL, Xu Q, Hu XY. Nickel metal–organic framework 2D nanosheets with enhanced peroxidase nanozyme activity for colorimetric detection of H_2O_2. Talanta. 2018;189:254–61.
5. Shu Y, Xu J, Chen JY, Xu Q, Xiao X, Jin DQ, Pang H, Hu XY. Ultrasensitive electrochemical detection of H_2O_2 in living cells based on ultrathin MnO_2 nanosheets. Sens Actuator B-Chem. 2017;252:72–8.
6. Shu Y, Li B, Xu Q, Gu P, Xiao X, Liu FP, Yu LY, Pang H, Hu XY. Cube-like $CoSn(OH)_6$ nanostructure for sensitive electrochemical detection of H_2O_2 in human serum sample. Sens Actuator B-Chem. 2017;241:528–33.
7. Cue Y, Chen F, Yin XB. A ratiometric fluorescence platform based on boric-acid-functional Eu-MOF for sensitive detection of H_2O_2 and glucose. Biosens Bioelectron. 2019;135:208–15.
8. Cowan EA, Taylor JL, Oldham CD, Dasari M, Doyle D, Murthy N, May SW. Cellular antioxidant activity of phenylaminoethyl selenides as monitored by chemiluminescence of peroxalate nanoparticles and by reduction of lipopolysaccharide-induced oxidative stress. Enzyme MicrobTechnol. 2013;53(6–7):373–77.
9. Chen JQ, Xue SF, Chen ZH, Zhang SQ, Shi GY, Zhang M. GelRed/$[G_3T]_5/Tb^{3+}$ hybrid: a novel label-free ratiometric fluorescent probe for H_2O_2 and oxidase-based visual biosensing. Biosens Bioelectron. 2018;100:526–32.
10. Pundir CS, Deswal R, Narwal V. Quantitative analysis of hydrogen peroxide with special emphasis on biosensors. Bioprocess Biosyst Eng. 2018;41(3):313–29.
11. Xu YQ, Li BH, Xiao LL, Ouyang J, Sun SG, Pang Y. A colorimetric and near-infrared fluorescent probe with high sensitivity and selectivity for acid phosphatase and inhibitor screening. Chem Commun. 2014;50(63):8677–80.
12. Shu Y, Ye QY, Dai T, Guan J, Ji ZP, Xu Q, Hu XY. Incorporation of perovskite nanocrystals into lanthanide metal–organic frameworks with enhanced stability for ratiometric and visual sensing of mercury in aqueous solution. J Hazard Mater. 2022;430:128360.
13. Shu Y, Dai T, Ye QY, Jin DQ, Xu Q, Hu XY. A dual-emitting two-dimensional nickel-based metal–organic framework nanosheets: Eu^{3+}/Ag^{+} functionalization synthesis and ratiometric sensing in aqueous solution. J Fluoresc. 2021;31(6):1947–57.
14. Shu Y, Ye QY, Dai T, Xu Q, Hu XY. Encapsulation of luminescent guests to construct luminescent metal–organic frameworks for chemical sensing. ACS Sensors. 2021;6(3):641–58.
15. Lee MH, Kim JS, Sessler JL. Small molecule-based ratiometric fluorescence probes for cations, anions, and biomolecules. Chem Soc Rev. 2015;44(13):4185–91.
16. Bigdeli A, Ghasemi F, Abbasi-Moayed S, Shahrajabian M, Fahimi-Kashani N, Jafarinejad S, Nejad MAF, Hormozi-Nezhad MR. Ratiometric fluorescent nanoprobes for visual detection: design principles and recent advances—a review. Anal Chim Acta. 2019;1079:30–58.

17. Zhang WT, Ren XY, Shi S, Li M, Liu LZ, Han XM, Zhu WX, Yue TL, Sun J, Wang JL. Ionic silver-infused peroxidase-like metal–organic frameworks as versatile "antibiotic" for enhanced bacterial elimination. Nanoscale. 2020;12(30):16330–8.
18. Chen W, Wu CS. Synthesis, functionalization, and applications of metal–organic frameworks in biomedicine. Dalton Trans. 2018;47(7):2114–33.
19. Zhao X, Wang YX, Li DS, Bu XH, Feng PY. Metal–Organic frameworks for separation. Adv Mater. 2018;30(37):1705189.
20. Ye K, Wang L, Song HW, Li X, Niu XH. Bifunctional MIL-53(Fe) with pyrophosphate-mediated peroxidase-like activity and oxidation-stimulated fluorescence switching for alkaline phosphatase detection. J Mater Chem B. 2019;7(31):4794–800.
21. Ruan XF, Liu D, Niu XH, Wang YJ, Simpson CD, Cheng N, Du D, Lin YH. 2D graphene oxide/Fe-MOF nanozyme nest with superior peroxidase-like activity and its application for detection of woodsmoke exposure biomarker. Anal Chem. 2019;91(21):13847–54.
22. Xu WQ, Jiao L, Yan HY, Wu Y, Chen LJ, Gu WL, Du D, Lin YH, Zhu CZ. Glucose oxidase-integrated metal–organic framework hybrids as biomimetic cascade nanozymes for ultrasensitive glucose biosensing. ACS Appl Mater Interfaces. 2019;11(25):22096–101.
23. Li SQ, Liu XD, Chai HX, Huang YM. Recent advances in the construction and analytical applications of metal–organic frameworks-based nanozymes. TrAC-Trends Anal Chem. 2018;105:391–403.
24. Ai LH, Li LL, Zhang CH, Fu J, Jiang J. MIL-53(Fe): a metal–organic framework with intrinsic peroxidase-like catalytic activity for colorimetric biosensing. Chem-Eur J. 2013;19(45):15105–8.
25. Gao CJ, Zhu HM, Chen J, Qiu HD. Facile synthesis of enzyme functional metal–organic framework for colorimetric detecting H_2O_2 and ascorbic acid. Chin Chem Lett. 2017;28(5):1006–12.
26. Guo JJ, Wu S, Wang Y, Zhao M. A label-free fluorescence biosensor based on a bifunctional MIL-101(Fe) nanozyme for sensitive detection of choline and acetylcholine at nanomolar level. Sens Actuators B Chem. 2020;312:128021.
27. Wang FQ, Chen L, Liu DH, Ma WR, Dramou P, He H. Nanozymes based on metal–organic frameworks: construction and prospects. TrAC-Trends Anal Chem. 2020;133:116080.
28. Niu XH, Li X, Lyu ZY, Pan JM, Ding SC, Ruan XF, Zhu WL, Du D, Lin YH. Metal–organic framework based nanozymes: promising materials for biochemical analysis. Chem Commun. 2020;56(77):11338–53.
29. Li SQ, Xiao DL, Liu DH, He H. Calcium-doped fluorescent carbon nanoparticles: spontaneous thermal synthesis, pH-sensitive fluorescence off-on, and mechanism. Sens Actuators B Chem. 2018;266:594–602.
30. Zuo PL, Lu XH, Sun ZG, Guo YH, He H. A review on syntheses, properties, characterization and bioanalytical applications of fluorescent carbon dots. Microchim Acta. 2016;183(2):519–42.
31. Falcaro P, Furukawa S. Doping light emitters into metal–organic frameworks. Angew Chem Int Ed. 2012;51(34):8431–3.
32. Fu QJ, Zhou XB, Wang MJ, Su XG. Nanozyme-based sensitive ratiometric fluorescence detection platform for glucose. Anal Chim Acta. 2022;1216:339993.
33. Zhang NN, Zhao LX, He MT, Luo P, Tan L. Assay of inorganic pyrophosphatase activity based on a fluorescence "turn-off" strategy using carbon quantum dots@Cu-MOF nanotubes. Spectrochim Acta A Mol Biomol Spectrosc. 2023;284:121771.
34. Lin RB, Li SM, Wang JY, Xu JP, Xu CH, Wang J, Li CX, Li ZQ. Facile generation of carbon quantum dots in MIL-53(Fe) particles as localized electron acceptors for enhancing their photocatalytic Cr(VI) reduction. Inorg Chem Front. 2018;5:3170–7.
35. Zhu S, Meng Q, Wang L, Zhang J, Song Y, Jin H, Zhang K, Sun H, Wang H, Yang B. Highly photoluminescent carbon dots for multicolor patterning, sensors, and bioimaging. Angew Chem Int Ed. 2013;52(14):3953–7.
36. Taylor-Pashow KML, Della Rocca J, Xie ZG, Tran S, Lin WB. Postsynthetic modifications of iron-carboxylate nanoscale metal–organic frameworks for imaging and drug delivery. J Am Chem Soc. 2009;131(40):14261–3.
37. Zhang Y, Yan B. A point-of-care diagnostics logic detector based on glucose oxidase immol/lobilized lanthanide functionalized metal–organic frameworks. Nanoscale. 2019;11(47):22946–53.
38. Geng NN, Chen W, Xu H, Ding MM, Lin T, Wu QS, Zhang L. Insights into the novel application of Fe-MOFs in ultrasound-assisted heterogeneous Fenton system: efficiency, kinetics and mechanism. Ultrason Sonochem. 2021;72:105411.
39. Liu P, Li X, Xu X, Ye K, Wang L, Zhu H, Wang M, Niu X. Integrating peroxidase-mimicking activity with photoluminescence into one framework structure for high-performance ratiometric fluorescent pesticide sensing. Sens Actuators B Chem. 2021;328:129024.
40. Zhou ZD, Zhao PC, Wan CX, Yan PP, Xie YX, Fe JJ. Ultra-sensitive amperometric determination of quercetin by using a glassy carbon electrode modified with a nanocomposite prepared from aminated graphene quantum dots, thiolated beta-cyclodextrin and gold nanoparticles. Microchim Acta. 2020;187(2):130.
41. Sheng ZH, Shao L, Chen JJ, Bao WJ, Wang FB, Xia XH. Catalyst-free synthesis of nitrogen-doped graphene via thermal annealing graphite oxide with melamine and its excellent electrocatalysis. ACS Nano. 2011;5(6):4350–8.
42. Li SQ, Hu X, Chen QM, Zhang XD, Chai HX, Huang YM. Introducing bifunctional metal–organic frameworks to the construction of a novel ratiometric fluorescence sensor for screening acid phosphatase activity. Biosens Bioelectron. 2019;137:133–9.
43. Xu XC, Luo ZJ, Ye K, Zou XB, Niu XH, Pan JM. One-pot construction of acid phosphatase and hemin loaded multifunctional metal–organic framework nanosheets for ratiometric fluorescent arsenate sensing. J Hazard Mater. 2021;412:124407.
44. Zhang WC, Li X, Xu XC, He YF, Qiu FX, Pan JM, Niu XH. Pd nanoparticle-decorated graphitic C_3N_4 nanosheets with bifunctional peroxidase mimicking and ON–OFF fluorescence enable naked-eye and fluorescent dual-readout sensing of glucose. J Mater Chem B. 2019;7(2):233–9.
45. Lei Y, Zhao W, Zhang Y, Jiang Q, He JH, Baeumner AJ, Wolfbeis OS, Wang ZL, Salama KN, Alshareef HN. A MXene-based wearable biosensor system for high-performance in vitro perspiration analysis. Small. 2019;15(19): e1901190.
46. Yan X, Li HX, Han XS, Su XG. A ratiometric fluorescent quantum dots based biosensor for organophosphorus pesticides detection by inner-filter effect. Biosens Bioelectron. 2015;74:277–83.